

Nonisothermal Crystallization of Isotactic Polypropylene Blended with Poly(α -pinene). I. Bulk Crystallization

MARIA LAURA DI LORENZO, SOSSIO CIMMINO, CLARA SILVESTRE

Istituto di Ricerca e Tecnologia delle Materie Plastiche (C.N.R.), Via Toiano 6, 80072 Arco Felice (NA), Italy

Received 11 May 2000; accepted 29 November 2000

ABSTRACT: The influence of a natural terpene resin, poly(α -pinene) (P α P), on the nonisothermal crystallization process of isotactic polypropylene (iPP) was investigated. The solidification process strongly depends on cooling rate, composition, and miscibility of the system. For the blends containing P α P up to 30 wt %, the overall nonisothermal crystallization rate is depressed with respect to plain iPP. This is probably the result of the diluting effect of the polyterpene because the two components are miscible. The 50/50 blend presents, instead, two amorphous phases: an iPP-rich phase and a P α P-rich phase. For this composition, solidification starts at temperatures higher than those for plain iPP and blends with lower P α P content, given that the diluting effect of P α P in the iPP-rich phase is counterweighted by an increased number of nuclei that originate from the polyterpene-rich phase domains. P α P also influences the morphology of iPP spherulites, which are spherical in plain iPP and become more irregular with increasing P α P content. The number and dimension of iPP spherulites depend on blend composition and miscibility of the components. Moreover, the nonisothermal crystallization kinetics of iPP/P α P blends was analyzed with the Ozawa equation. © 2001 John Wiley & Sons, Inc. *J Appl Polym Sci* 82: 358–367, 2001

Key words: nonisothermal crystallization; isotactic polypropylene; polyterpene; poly(α -pinene); blend; nucleation; Ozawa equation

INTRODUCTION

Isotactic polypropylene (iPP) is a thermoplastic material widely used in several sectors because it offers interesting combinations of good mechanical performance, heat resistance, fabrication flexibility, and low cost. It is one of the most used polymers in the food packaging sector, in spite of its relatively high permeability to oxygen compared to that of other plastic materials, for example, nylon, poly(vinyl chloride), poly(ethylene terephthalate), poly(ethylene-co-vinyl alcohol), and poly(vinylidene chloride).¹ Several studies have

thus been directed to decrease the diffusion of gases through iPP films. One of the approaches consists in the addition of a second component to iPP to improve its barrier properties.

To produce ecosustainable iPP-based materials for food packaging, oligomers of natural terpene resins have been suggested as possible additives to iPP.^{2,3} Preliminary studies have shown that some polyterpenes, that is, poly(α -pinene) (P α P) and polylimonene, can successfully decrease the permeability of iPP to gases.³ Miscibility, phase structure, and isothermal crystallization process of iPP blended with the amorphous poly(α -pinene) (P α P) have been investigated in detail.^{2,4,5} These studies suggested a partial miscibility of the components with the presence of an upper critical solution temperature (UCST).²

Correspondence to: M. L. Di Lorenzo (diloren@irtemp.na.cnr.it).

Journal of Applied Polymer Science, Vol. 82, 358–367 (2001)
© 2001 John Wiley & Sons, Inc.

When the blends crystallize from the melt at temperatures above the UCST and then are cooled to room temperature, the resulting amorphous phase is homogeneous because the presence of the crystallites prevents the liquid–liquid phase separation.^{2,5,6} When iPP/P α P blends are cooled from the melt at 10°C/min, the amorphous phase remains homogeneous for samples with up to 30 wt % P α P, whereas the 50/50 blend separates into an iPP-rich phase and a P α P-rich phase.⁵ A more rapid cooling (i.e., from 210°C to room temperatures in about 2 min) also induces phase separation for the 70/30 blend.²

Previous studies of isothermal crystallization kinetics of iPP/P α P blends with various compositions showed that the addition of resin up to 30 wt % causes, at the same crystallization temperature, a decrease of the radial growth rate of spherulites and of the overall solidification rate.⁴ However, crystallization during processing operations of polymers almost invariably occurs under nonisothermal conditions. This raises the question of how solidification rates measured at constant temperatures can be applied to nonisothermal processes.

It is known that the conditions under which a polymer solidifies from the melt determine the crystalline structure and morphology, and thus the properties of a material. Therefore, to reach the optimum conditions for industrial processes and to obtain products with tailored properties, it is necessary to have quantitative evaluations of nonisothermal crystallization rates.⁷

Studies of nonisothermal crystallization of plain iPP were performed by several authors. Monasse and Haudin⁸ studied the thermal dependence of nucleation and growth rate, and found a transition from heterogeneous to homogeneous nucleation at about 122°C. Similarly, Lim et al.^{9,10} and Eder and Wlochowicz,¹¹ showed that iPP crystallization proceeds through heterogeneous nucleation with three-dimensional growth of the crystallites, and that at low temperatures homogeneous nucleation occurs.

The dependence of iPP polymorphism on cooling rate was investigated by Piccarolo and co-workers.^{12–14} At cooling rates lower than 10–20°C/s only the α -monoclinic phase forms, above 200°C/s only the metastable phase develops, and between 20 and 200°C/s smectic and α -monoclinic phases coexist. Solidification at these intermediate cooling rates leads to compe-

titition between monoclinic and smectic forms, the latter prevailing at higher cooling rates.

Burfield et al.¹⁵ analyzed the dependence of the thermal properties of polypropylene on tacticity and catalyst system used for the synthesis. The crystallization onset temperature decreases with reduced isotacticity and, at a given tacticity, polymers prepared from supported catalysts present lower crystallization temperatures. A similar study was conducted by Paukkeri and Lehtinen,¹⁶ who proved that isotacticity is the main parameter determining the crystallization peak temperature and crystallinity, whereas molecular mass has a much less pronounced effect on solidification rates and almost no influence on crystallinity.

The dynamic crystallization process of iPP in the presence of various nucleating substances was studied by several authors, for example, Lim et al.,^{9,10} Feng et al.,¹⁷ Zhang et al.,¹⁸ Cazé et al.,¹⁹ and Bogoeva–Gaceva et al.²⁰

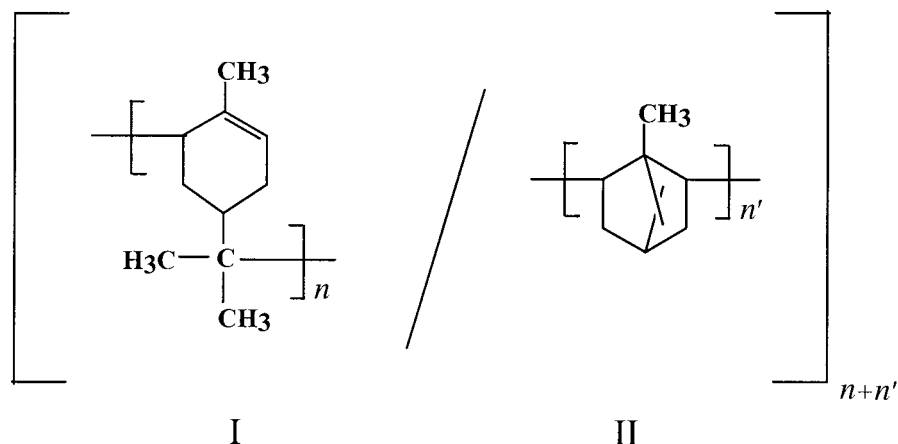
The objective of our study is to investigate the effect of P α P on overall nonisothermal crystallization of iPP. iPP/P α P blends were prepared by melt mixing and compression molding. No thermal degradation of isotactic polypropylene has been reported to occur below 230–250°C,²¹ which is well above the temperatures used for the processing of the blends. As the addition of P α P stabilizes iPP against thermal degradation,³ it is safe to exclude any thermal degradation during both preparation and nonisothermal cooling of the blends.

EXPERIMENTAL

Materials

The isotactic polypropylene (iPP) was a commercial product, Shell HY 6100, kindly supplied by Montell Polyolefins (Ferrara, Italy), with $M_w = 3.0 \times 10^5 \text{ g mol}^{-1}$. The poly(α -pinene) (P α P) was a commercial resin, kindly supplied by Hercules (Rijswijk, The Netherlands). P α P is an amorphous oligomer derived from the polymerization of α -pinene monoterpene, which is the main constituent of the wood of coniferous plants. The sample used was Piccolyte A115, with softening point = 115°C (Ring and Ball method), $T_g = 61^\circ\text{C}$, $M_n = 680 \text{ g mol}^{-1}$, $M_w = 1075 \text{ g mol}^{-1}$, and $M_z = 1650 \text{ g mol}^{-1}$ (Hercules data).

The structure of P α P is not exactly known. Its main chain probably consists of two repeat units, as shown below^{22,23}:



Blend Preparation

Binary blends of polyolefin/resin were obtained by mixing the iPP and P α P components in a Bra-bender-like apparatus (Rheocord EC; Haake Inc., Paramus, NJ) at 210°C and 32 rpm for 10 min. The mixing ratios of iPP/resin (w/w) were: 100/0, 90/10, 80/20, 70/30, and 50/50.

Preparation of Compression-Molded Samples

The mixed material was compression-molded in a heated press at a temperature of 210°C for 5 min, without any applied pressure, to allow complete melting. After this period, a pressure of 100 bar was applied for 5 min. Next, the plates of the press, containing coils for fluids, were rapidly cooled to room temperature by cold water, then pressure was released and the mold removed from the plates. Films of 150 μ m thickness were produced.

Thermal Analysis

A differential scanning calorimeter (Mettler DSC 30) was used to investigate the nonisothermal crystallization of the compression-molded iPP/P α P samples. The apparatus was calibrated with pure indium, lead, and zinc standards at various scanning rates.

Each sample was heated from 30 to 200°C at the rate of 30°C/min, kept at this temperature for 10 min to allow complete melting, and then cooled to room temperature at five different scanning rates: 0.5, 1, 2, 4, and 8°C/min. Each experiment was repeated three times to ensure reproducibility. Dry nitrogen gas with a flow rate of 20 mL min⁻¹ was purged through the cell.

Optical Microscopy

The morphology of the iPP/P α P blends was investigated by optical microscopy, using a Zeiss polarizing microscope equipped with a hot stage. The compression-molded films, squeezed between two microscope glasses, were heated from 30 to 200°C at 30°C/min, kept at this temperature for 10 min to allow complete melting, and then cooled to room temperature at 4°C/min. Dry nitrogen gas was purged through the hot stage.

RESULTS AND DISCUSSION

The analysis of polymer crystallization in nonisothermal conditions by calorimetric methods must be performed with care because it is complicated by the possible occurrence of thermal gradients within the sample and between the cooling furnace and the sample. For thin specimens (\approx 0.3 mm) and for scanning rates that do not exceed 80°C/min, the latter factor is of little importance.⁸ The former factor, instead, is more critical and its occurrence needs to be limited by choosing appropriate experimental conditions. In the absence of transitions, to avoid thermal gradients scanning rates should not exceed 1 and 100°C/min for samples of 1 g and 1 mg, respectively.²⁴

In addition, crystallization is an exothermic process and the heat developed during the phase transition may cause some local heating and create additional thermal gradients within the sample. As a consequence, transitions can occur at temperatures that do not correspond to those detected by the instrumentation. The thicker the sample, the more critical this problem is.

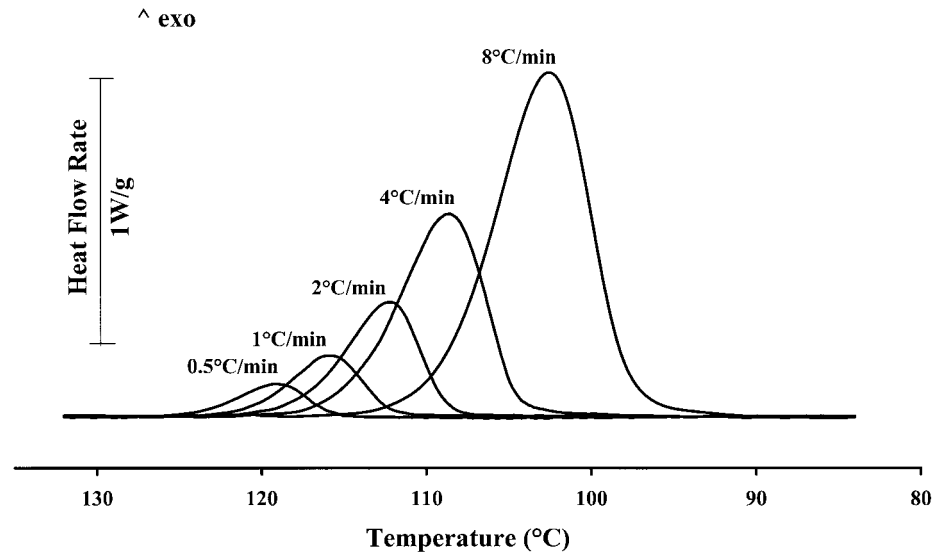


Figure 1 Heat flow rate of iPP/P α P 90/10 blend cooled at various scanning rates.

To limit the problems arising from thermal lags, for the present analysis the scanning rate was limited to 8°C/min, and 0.15-mm-thick samples of approximately 3 mg were used.

The results obtained studying the nonisothermal solidification process of iPP/P α P blends showed that the mechanism of phase change depends on cooling rate and composition. For every composition, with increasing cooling rate χ , the crystallization curves shift to lower temperatures, as shown in Figure 1 for the 90/10 blend. At lower χ there is more time to overcome the nucleation

barrier, so crystallization starts at higher temperatures, whereas at higher χ nuclei become active at lower temperatures.⁷

The influence of P α P on dynamic solidification of iPP is shown in Figure 2, which presents the thermoanalytical curves of iPP/P α P blends crystallized at $\chi = 4^\circ\text{C}/\text{min}$. Similar trends were obtained for the other cooling rates. The addition of P α P up to 30 wt % shifts the crystallization curves to lower temperatures. This effect indicates that in the presence of P α P, iPP needs higher undercooling to crystallize. When 50% of

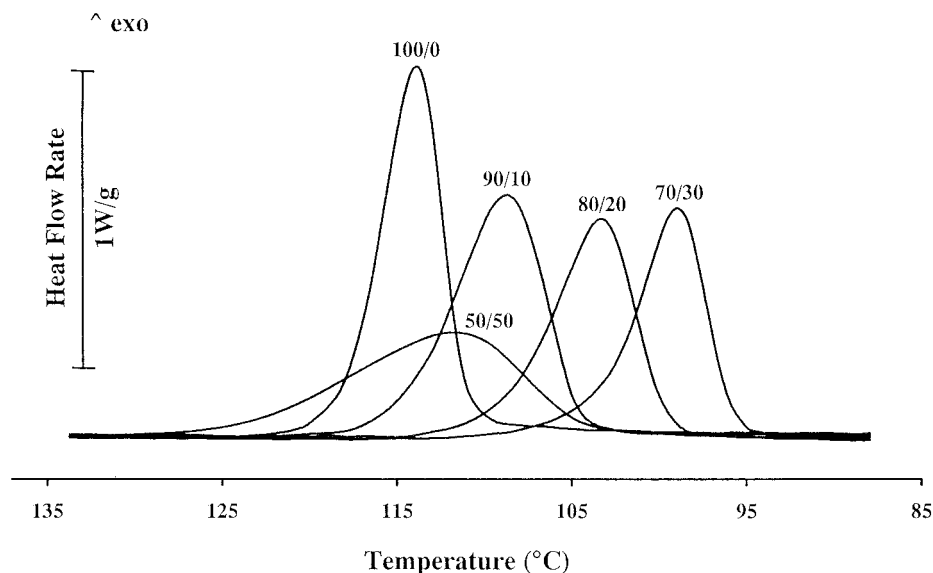


Figure 2 Heat flow rate of iPP/P α P blends cooled at 4°C/min.

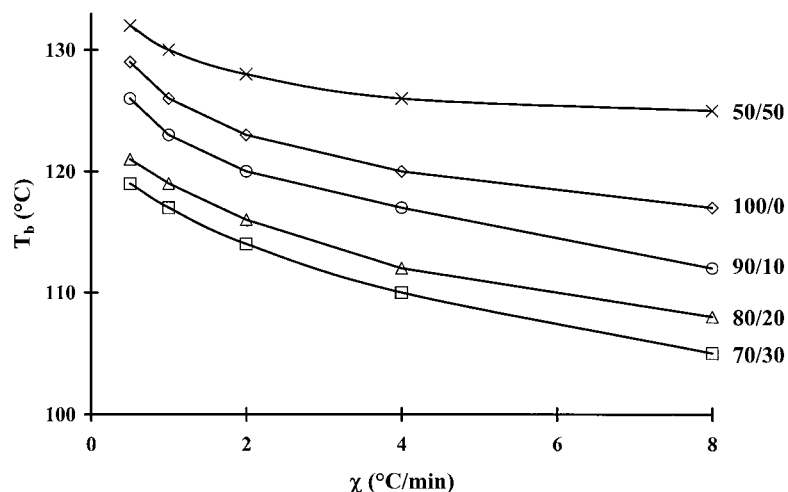


Figure 3 Onset temperature of crystallization of iPP/P α P blends as a function of cooling rate.

P α P is added to iPP, crystallization starts at a temperature higher than that of plain iPP, and the curve is much broader.

From the solidification exotherms, the onset temperature T_b and the temperature corresponding to the maximum of the peak T_p were measured and are shown in Figures 3 and 4, respectively. Both T_b and T_p depend on cooling rate and composition. At all the cooling rates used, for the blends containing up to 30% P α P, a decrease of T_b and T_p with the addition of polyterpene is observed. For the 50/50 blend, for all the cooling rates used, T_b values were always higher than those of iPP and blends with lower P α P content, as shown in Figure 3. The T_p of the 50/50 blend

was slightly lower than that of iPP, but higher than that of the other blends examined (Fig. 4).

These results can be accounted for by examining the phase structure of the blends as a function of composition. Previous studies showed that in the range of temperatures at which nonisothermal crystallization occurs, the 90/10, 80/20, and 70/30 iPP/P α P blends have one homogeneous amorphous phase, whereas the 50/50 blend presents liquid-liquid phase separation, with the formation of an iPP-rich phase and a P α P-rich phase.^{2,5} For the blends with P α P content up to 30 wt %, the decrease of solidification rate can be attributed mainly to the diluting effect of P α P. As a consequence, crystallization starts at lower

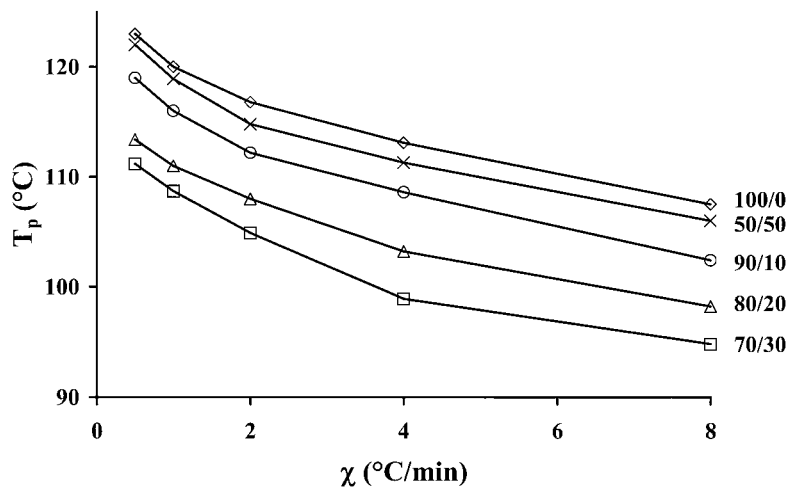


Figure 4 Maximum of crystallization peak of iPP/P α P blends as a function of cooling rate.

temperatures. In the phase-separated 50/50 blend, the presence of the dispersed phase probably lowers the activation energy required for the formation of stable nuclei, allowing the crystallization process to start at lower undercooling. The increased broadness of the transition in the 50/50 sample is to be ascribed to the low value of spherulite growth rate.²⁵

Nucleation in iPP/P α P blends was investigated by optical microscopy. Figure 5 shows the optical micrographs of plain iPP and iPP/P α P samples crystallized at 4°C/min. Polypropylene solidifies according to a prevalent spherulitic morphology. For the blends, the spherulite number and dimension strongly depend on composition. In iPP and 90/10 samples cooled at 4°C/min, large and small spherulites, nucleated at different times and temperatures, are present [Fig. 5(a) and (b)]. During cooling from the melt, a few nuclei form, giving rise to large spherulites. At lower temperatures, many other nuclei suddenly appear. As their number is elevated, they quickly impinge each other, forming small spherulites. For the 80/20 and 70/30 blends only one type of spherulite is formed [Fig. 5(c) and (d)]. The total number of spherulites in the blends with a homogeneous amorphous phase, that is, with P α P up to 30%, diminishes with increasing P α P content as a result of the dilution of nuclei by P α P.

In the iPP/P α P 50/50 blend, many nuclei start to grow at high temperatures, giving rise to a large number of small spherulites, as exhibited in Figure 5(e). In phase-separated blends, increase of nucleation density is often explained with migration of heterogeneities from one component to the other.^{26–28} This should not be the case for iPP/P α P blends because for the blends with a single amorphous phase, diminution of nucleation density with P α P content is observed. In the phase-separated 50/50 blend, heterogeneous nuclei are probably formed at the interfaces between the dispersed particles and the iPP-rich phase matrix. Such a nucleation mechanism has been shown to occur in other phase-separated binary blends of iPP in which the second component is in rubbery state, like blends of iPP with atactic polystyrene²⁸ and blends of iPP with *trans*-polyoctenylene.²⁹ The activity of the interface toward primary nucleation of crystallization of the matrix is probably attributable to a decrease of the energy barrier for the formation of heterogeneous nuclei contacting with the interface.²⁸ In the iPP/P α P 50/50 blend, these heterogeneous nuclei favor crystallization of iPP, which starts at higher tem-

peratures compared to that of iPP and to iPP/P α P blends with one homogeneous amorphous phase (see Fig. 3).

To analyze the kinetic parameters of the non-isothermal crystallization process, the method proposed by Ozawa³⁰ was applied. According to Ozawa, the degree of conversion at temperature T is related to the cooling rate χ by the expression

$$X(T) = 1 - e^{-[K(T)/\chi^n]} \quad (1)$$

where $X(T)$ is the relative crystallinity at temperature T , n is the Avrami exponent, and $K(T)$ is the cooling crystallization function. K is related to the overall crystallization rate and indicates how fast crystallization occurs.³¹ Equation (1) can be rewritten as

$$\log\{-\ln[1 - X(T)]\} = \log[K(T)] - n \log(\chi) \quad (2)$$

By plotting the left term of eq. (2) against $\log(\chi)$, a straight line should be obtained and the kinetic parameters K and n can be derived from the slope and the intercept, respectively. Previous investigations showed that this method can be applied to analyze the dynamic solidification of plain iPP.^{8,9,11,32}

In Figure 6 the $\log\{-\ln[1 - X(T)]\}$ versus $\log(\chi)$ plots for two iPP/P α P blends are shown. Experimental data for these two blends, as well as those (not shown) of plain iPP and of the other blends, were fitted by straight lines. Thus the Ozawa equation seems to satisfactorily describe the nonisothermal crystallization of iPP/P α P blends.

Intercepts of the Ozawa plots provide the cooling crystallization function K . Plots of $\log(K)$ as a function of temperature are reported in Figure 7. For iPP/P α P blends with P α P content up to 30%, the value of $\log(K)$ decreases with the increase of polyterpene amounts. For all the compositions, $\log(K)$ is a decreasing linear function of T , as observed for other polymers.^{11,33,34} For the miscible blends, the diminution of K with temperature follows the trend of both nucleation and growth rates. For the 50/50 blend, the dependence of K on temperature is much lower because the nucleation rate, which is mainly heterogeneous, changes little with T , and the decrease of K with temperature is caused only by the variation of growth rate. Moreover, K values of the 50/50 blend lie between those of plain iPP and 90/10 blend. This behavior can be accounted for by the presence of P α P-rich phase droplets in the melt that act as

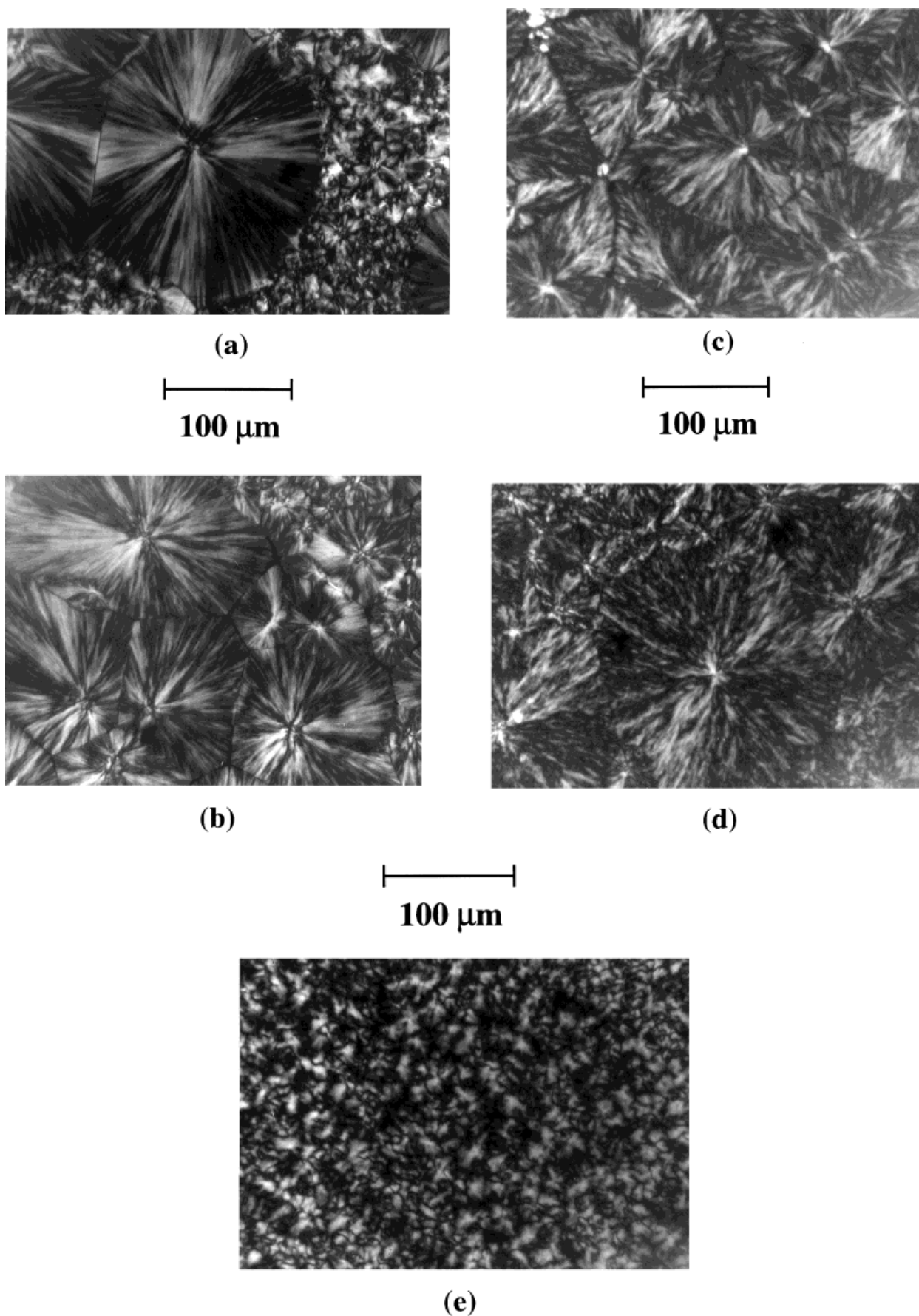


Figure 5 Optical micrographs of iPP/PαP blends crystallized at 4°C/min: (a) 100/0; (b) 90/10; (c) 80/20; (d) 70/30; (e) 50/50.

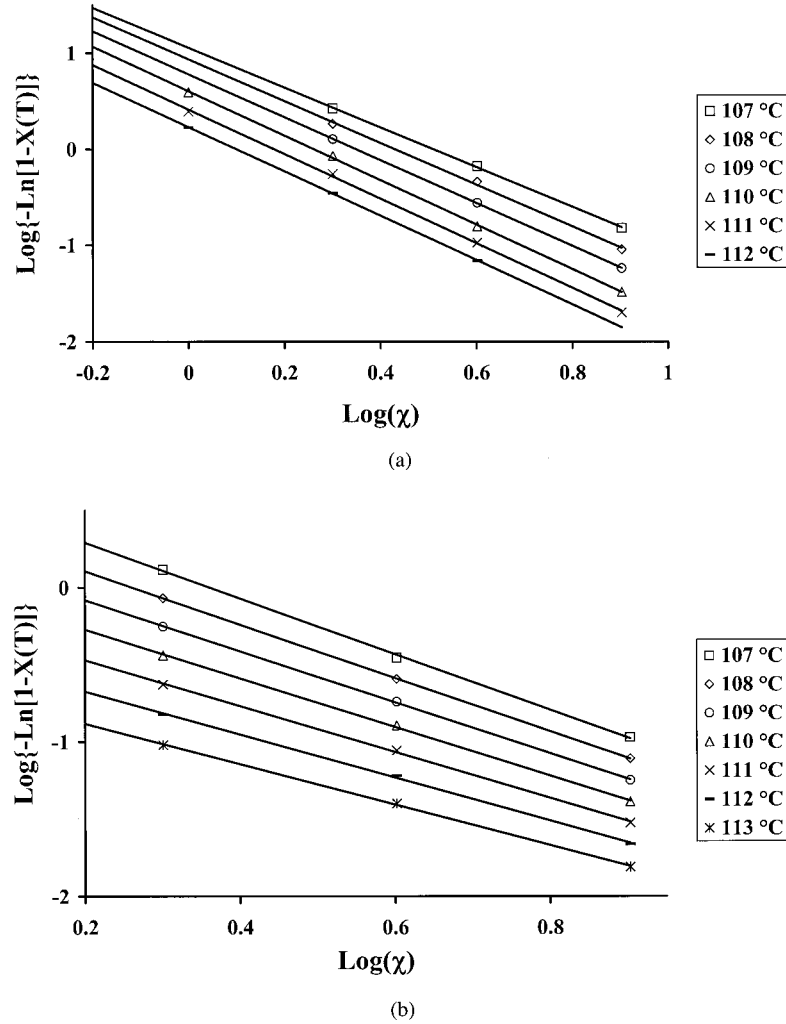


Figure 6 Ozawa plot of iPP/P α P blends: (a) 80/20; (b) 70/30.

nucleation surfaces for solidification, thus accelerating the crystallization.

Values of the Avrami exponent are reported in Table I. For plain iPP, n lies between 3 and 4, in

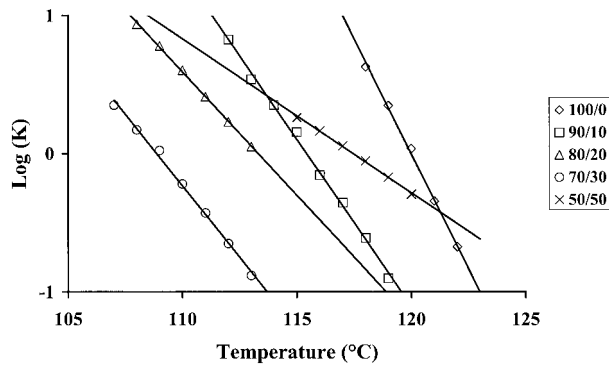


Figure 7 Cooling crystallization function versus temperature plot of iPP/P α P blends.

agreement with the data reported in the literature for crystallization conducted in isothermal and nonisothermal conditions,^{8,9,11,32,35,36} indicating that iPP crystals grow from both homogeneous and heterogeneous nuclei.

The addition of P α P to iPP produces a decrease of the Avrami exponent, suggesting a change in the nucleation mechanism and/or in the morphology of the spherulites. A lower value of the Avrami exponent with the presence of P α P was also documented for isothermal crystallization, where n was found close to 3 for iPP and close to 2 for the blends with P α P up to 30%, indicating three-dimensional and bidimensional growths, respectively, supposing heterogeneous nucleation.⁴ P α P influences the morphology of iPP spherulites: with increasing P α P content in the blend, the formation of spherulites with irregular growth face can be observed (see Fig. 5). The

Table I Values of Avrami Exponent for iPP/P α P Blends Determined by Ozawa Equation

Temperature (°C)	iPP/P α P Blend				
	100/0	90/10	80/20	70/30	50/50
106				1.9	
107				1.8	
108			2.0	1.7	
109			2.2	1.7	
110			2.2	1.6	
111			2.3	1.5	
112		2.5	2.3	1.4	
113		2.4	2.3		
114		2.5	2.4		
115		2.6			1.2
116		2.6			1.2
117		2.6			1.3
118	3.3	2.8			1.4
119	3.4	3.0			1.4
120	3.3				1.5
121	3.2				
122	3.3				
123	3.4				

irregularity of the shape of iPP spherulites in the blends increases with the addition of P α P, although their appearance remains roughly spherical. Therefore, the Avrami index does not seem able to explain the crystallization mechanism in the case of iPP/P α P blends. This probably occurs because the equation used does not take into account that, during the growth, the crystallizable molecules have to deviate to englobe, deform, and/or reject the noncrystallizable component.

CONCLUSIONS

The analysis of the nonisothermal crystallization process of iPP/P α P binary blends has shown that the solidification behavior of the system is strongly influenced by the miscibility of the components. For the miscible blends (90/10, 80/20, and 70/30), the addition of P α P retards the solidification of iPP as a consequence of the diluting effect of P α P. For the phase-separated blend (50/50), the droplets of the P α P-rich phase act as nucleation promoters for iPP crystallization. In these conditions, solidification starts at temperatures even higher than those for plain iPP because of the increased nucleation temperature,

although crystallization proceeds very slowly because of the high dilution.

P α P also influences the morphology of iPP spherulites, which become irregular with increasing P α P content. Their number and dimension depend on composition and miscibility of the blends: P α P produces a dilution of nuclei in the blends that present one homogeneous amorphous phase, whereas in the phase-separated blend the particles of the dispersed phase generate an increase in nucleation density.

The authors warmly thank G. Loeber of the Hercules International Ltd. Co. (The Netherlands) for kindly supplying the poly(α -pinene). The authors also wish to thank Prof. P. Geil (University of Illinois) for carefully reviewing the manuscript. This work was partially supported by P.O.P. 1994/1999 Regione Campania, Sottoprogramma 5, Azione 5.4.2, and Annualità 1997, Enti Pubblici di Ricerca.

REFERENCES

1. Silvis, H. C. *Trends Polym Sci* 1997, 5, 75.
2. Cimmino, S.; D'Alma, E.; Di Lorenzo, M. L.; Di Pace, E.; Silvestre, C. *J Polym Sci Part B Polym Phys* 1999, 37, 867.
3. Cimmino, S.; D'Alma, E.; Di Lorenzo, M. L.; Greco, R.; Iavarone, M.; Silvestre, C., in preparation.
4. Silvestre, C.; Cimmino, S.; D'Alma, E.; Di Lorenzo, M. L.; Di Pace, E. *Polymer* 1999, 40, 5119.
5. Di Lorenzo, M. L.; Cimmino, S.; Orsello, G.; Pyda, M.; Silvestre, C.; Wunderlich, B., in preparation.
6. Cimmino, S.; Iodice, P.; Martuscelli, E.; Silvestre, C. *Thermochim Acta* 1998, 321, 89.
7. Di Lorenzo, M. L.; Silvestre, C. *Prog Polym Sci* 1999, 24, 917.
8. Monasse, B.; Haudin, J. M. *Colloid Polym Sci* 1986, 264, 117.
9. Lim, G. B. A.; Lloyd, D. R. *Polym Eng Sci* 1993, 33, 529.
10. Lim, G. B. A.; McGuire, K. S.; Lloyd, D. R. *Polym Eng Sci* 1993, 33, 537.
11. Eder, M.; Wlochowicz, A. *Polymer* 1983, 24, 1593.
12. Piccarolo S. *J Macromol Sci Phys* 1992, B31, 501.
13. Piccarolo, S.; Saiu, M.; Brucato, V.; Titomanlio, G. *J Appl Polym Sci* 1992, 46, 625.
14. Sondergaard, K.; Minà, P.; Piccarolo, S. *J Macromol Sci Phys* 1997, B36, 733.
15. Burfield, D. R.; Loi, P. S. T.; Doi, Y.; Mejzík, J. *J Appl Polym Sci* 1990, 41, 1095.
16. Paukeri, R.; Lehtinen, A. *Polymer* 1993, 34, 4075.
17. Feng, Y.; Jin, X.; Hay, J. N. *J Appl Polym Sci* 1998, 69, 2089.
18. Zhang, R.; Zheng, H.; Lou, X.; Ma, D. *J Appl Polym Sci* 1994, 51, 51.

19. Cazé, C.; Devaux, E.; Crespy, A.; Cavrot, J. P. *Polymer* 1997, 38, 497.
20. Bogoeva-Gaceva, G.; Janevski, A.; Grozdanov, A. *J Appl Polym Sci* 1998, 67, 395.
21. Vasile, C. in *Handbook of Polyolefins*, 2nd ed.; Vasile, C., Ed.; Marcel Dekker: New York, 2000; pp. 413–476.
22. Higashimura, T.; Lu, J.; Kamigaito, M.; Sawamoto, M. *Makromol Chem* 1993, 194, 3441.
23. Lu, J.; Kamigaito, M.; Sawamoto, M.; Higashimura, T.; Deng, Y. *J Appl Polym Sci* 1996, 61, 1011.
24. Wunderlich, B. in *Thermal Characterization of Polymeric Materials*, 2nd ed.; Turi, E., Ed.; Academic Press: New York, 1997; Chapter 2, pp. 205–482.
25. Di Lorenzo, M. L.; Cimmino, S.; Silvestre, C. *Macromolecules* 2000, 33, 3828.
26. Galeski, A.; Bartczak, Z.; Pracella, M. *Polymer* 1984, 28, 1323.
27. Bartczak, Z.; Martuscelli, E.; Galeski, A. in *Polypropylene: Structure, Blends and Composites*; Karger-Kocsis, J., Ed.; Chapman & Hall: London, 1995; Vol. 2, Chapter 2, pp. 25–49.
28. Bartczak, Z.; Galeski, A.; Krasnikova, N. P. *Polymer* 1987, 28, 1627.
29. Wenig, W.; Fiedel, H. W. *Makromol Chem* 1991, 192, 191.
30. Ozawa, T. *Polymer* 1971, 12, 150.
31. López, L. C.; Wilkens, G. L. *Polymer* 1989, 30, 882.
32. Hammami, A.; Spruiell, J. E.; Mehrotra, A. K. *Polym Eng Sci* 1995, 35, 797.
33. Kostov, G.; Bogadanov, B.; Nikolov, A. J. *J Therm Anal* 1994, 41, 925.
34. Silvestre, C.; Cimmino, S.; Di Lorenzo, M. L. *J Appl Polym Sci* 1999, 71, 1677.
35. Wunderlich, B. *Macromolecular Physics: Crystal Nucleation, Growth, and Annealing*, Vol. 2; Academic Press: New York, 1976.
36. Silvestre, C.; Di Lorenzo, M. L.; Di Pace, E. in *Handbook of Polyolefins*; Vasile, C., Ed.; Marcel Dekker: New York, 2000; Chapter 9, pp. 223–248.